MAY 27 1997

SANDIA REPORT
SAND97-0804 • UC-400
Unlimited Release
Printed May 1997

In-Situ Spectral Reflectance for Improving Molecular Beam Epitaxy Device Growth

RECEIVED
JUN 0 1 1997
OSTI

W. G. Breiland, B. E. Hammons, H. Q. Hou, K. P. Killeen, J. F. Klem, J. L. Reno, M. Sherwin

Prepared by
Sandia National Laboratories
Albuquerque, New Mexico 87185 and Livermore, California 94550

Sandia is a multiprogram laboratory operated by Sandia Corporation, a Lockheed Martin Company, for the United States Department of Energy under Contract DE-AC04-94AL85000.

MASTER

Approved for public release; distribution is unlimited.

DISTRIBUTION OF THIS DOCUMENT IS UNLIMITED

SF2900Q(8-81)

Issued by Sandia National Laboratories, operated for the United States Department of Energy by Sandia Corporation.

NOTICE: This report was prepared as an account of work sponsored by an agency of the United States Government. Neither the United States Government nor any agency thereof, nor any of their employees, nor any of their contractors, subcontractors, or their employees, makes any warranty, express or implied, or assumes any legal liability or responsibility for the accuracy, completeness, or usefulness of any information, apparatus, product, or process disclosed, or represents that its use would not infringe privately owned rights. Reference herein to any specific commercial product, process, or service by trade name, trademark, manufacturer, or otherwise, does not necessarily constitute or imply its endorsement, recommendation, or favoring by the United States Government, any agency thereof, or any of their contractors or subcontractors. The views and opinions expressed herein do not necessarily state or reflect those of the United States Government, any agency thereof, or any of their contractors.

Printed in the United States of America. This report has been reproduced directly from the best available copy.

Available to DOE and DOE contractors from
Office of Scientific and Technical Information
P.O. Box 62
Oak Ridge, TN 37831

Prices available from (615) 576-8401, FTS 626-8401

Available to the public from
National Technical Information Service
U.S. Department of Commerce
5285 Port Royal Rd
Springfield, VA 22161

NTIS price codes
Printed copy: A03
Microfiche copy: A01

DISCLAIMER

This report was prepared as an account of work sponsored by an agency of the United States Government. Neither the United States Government nor any agency thereof, nor any of their employees, make any warranty, express or implied, or assumes any legal liability or responsibility for the accuracy, completeness, or usefulness of any information, apparatus, product, or process disclosed, or represents that its use would not infringe privately owned rights. Reference herein to any specific commercial product, process, or service by trade name, trademark, manufacturer, or otherwise does not necessarily constitute or imply its endorsement, recommendation, or favoring by the United States Government or any agency thereof. The views and opinions of authors expressed herein do not necessarily state or reflect those of the United States Government or any agency thereof.

DISCLAIMER

Portions of this document may be illegible in electronic image products. Images are produced from the best available original document.

SAND97-0804
Unlimited Release
Printed May 1997

Distribution
Category UC-400

In-Situ Spectral Reflectance for Improving Molecular Beam Epitaxy Device Growth

LDRD Project 3505410000

W. G. Breiland
Chemical Processing Sciences Dept.
Sandia National Laboratories
P.O. Box 5800
Albuquerque, NM 87185-0601

LDRD participants: W. G. Breiland, B. E. Hammons, H. Q. Hou, K. P. Killeen, J. F. Klem, J. L. Reno, and M. Sherwin

Abstract

This report summarizes the development of *in situ* spectral reflectance as a tool for improving the quality, reproducibility, and yield of device structures grown from compound semiconductors. Although initially targeted at MBE (Molecular Beam Epitaxy) machines, equipment difficulties forced us to test most of our ideas on a MOCVD (Metal Organic Chemical Vapor Deposition) reactor. A pre-growth control strategy using *in situ* reflectance has led to an unprecedented demonstration of process control on one of the most difficult device structures that can be grown with compound semiconductor materials. Hundreds of vertical cavity surface emitting lasers (VCSEL's) were grown with only ± 0.3% deviations in the Fabry-Perot cavity wavelength – a nearly ten-fold improvement over current calibration methods. The success of the ADVISOR (Analysis of Deposition using Virtual Interfaces and Spectroscopic Optical Reflectance) method has led to a great deal of interest from the commercial sector, including use by Hewlett Packard and Honeywell. The algorithms, software and reflectance design are being evaluated for patents and/or license agreements. A small company, Filmetrics, Inc., is incorporating the ADVISOR analysis method in its reflectometer product.

DISTRIBUTION OF THIS DOCUMENT IS UNLIMITED

Contents

INTRODUCTION — *3*

Motivations for Project — 3

MBE (Molecular Beam Epitaxy) — 3

CVD (Chemical Vapor Deposition) and MOCVD (Metal-Organic Chemical Vapor Deposition) — 5

Approach — 6

Description of the ADVISOR method — 7

The Virtual Interface Concept — 7

Growth Rate Extraction — 8

RESULTS — *9*

Sensitivity Studies — 9

Monte Carlo Simulations — 9

Sensitivity Studies on HFET's and DBR (Distributed Bragg Reflectors) — 10

ADVISOR Application to MBE growth — 10

ADVISOR Application to the Growth of VCSEL's — 11

Apparatus — 11

Thin Film requirements for VCSEL Growth — 12

General AlAs and GaAs Growth Behavior — 13

Etchback Growth Behavior — 14

Specific Calibration Scheme for 845 nm and 770 nm VCSEL's — 14

Real Time Growth Monitor — 15

SUMMARY — *17*

PUBLICATIONS — *17*

Appendix: Thin film reflectance physics and the ADVISOR method — *19*

Maxwell equations at an interface — 19

General Expression for Multiple-layer Thin Film Reflectance — 22

Virtual interface model — 22

Extraction of growth rate and optical constants: The ADVISOR method — 25

INTRODUCTION

This report summarizes the development of *in situ* spectral reflectance as a tool for improving the quality, reproducibility, and yield of device structures grown from compound semiconductors. The goal of this program was to develop a technique to improve our capability to grow selected device structures with critical epilayer tolerances. The target devices for this effort were self-aligned gate field effect transistors (FETs), and vertical-cavity surface-emitting lasers (VCSELs). The FET devices are challenging by virtue of their high degree of threshold voltage sensitivity with respect to channel-to-gate distance, which requires nanometer-level control of epilayer thickness. Similarly, the VCSELs are very dependent on precise layer thicknesses and compositions to align the wavelengths of maximum mirror stack reflectivity, Fabry-Perot cavity resonance, and maximum active region gain. These two device structures exemplify the extremes of device design: the FET with a relatively simple epilayer structure requiring high absolute precision in the growth of very thin layers, and the VCSEL with a very complicated structure requiring tight fractional tolerances on relatively thick layers.

The project was originally targeted for molecular beam epitaxy applications. However, delays in operation of the equipment forced us to transfer a bulk of the experimental verification to a metal-organic chemical vapor deposition system. The methods developed in the project are generally applicable to either kind of deposition system.

Below is a summary of the motivations driving the goals of this project. This is followed by a general description of the approach taken to achieve these goals. Finally, summaries of the theoretical and experimental results of the research are given.

Motivations for Project

MBE (Molecular Beam Epitaxy)

The evolution of molecular beam epitaxy (MBE) crystal growth technology has resulted in machines capable of producing material with excellent uniformity, very low surface defect densities, and high throughput. Compared to first-generation machines, current designs also possess improved short-term effusion cell flux stability, which translates directly into short-term epilayer thickness and composition stability. Unfortunately, the demands of high uniformity and low defect densities result in machine designs which tend to sacrifice long-term flux stability, primarily as a result of effusion cell material depletion. For example, one MBE equipment manufacturer currently specifies a growth rate decrease of ~2% per 10μm of material grown. In addition, the flux stability of some sources, such as Al, is inherently poor due to effects such as crucible wetting or surface area variations. Because these effects are generally very difficult to model or predict, periodic calibrations of growth rates are generally performed *in situ* by a technique such as reflection high-energy electron diffraction (RHEED), or *ex situ* by a variety of techniques. Either of these methods requires recalibration at a frequency directly related to the desired accuracy of growth, which may mean as often as every day for critical device structures.

In addition, neither of these approaches allows for true real-time closed-loop control of the growth process.

Compounding the problem are the increasing demands which sophisticated device designs place on the growth process. In some cases, device processing is simplified by eliminating steps which once were used to compensate for loose tolerances on epitaxial material parameters. In other cases, close tolerances on the epilayer structure are the only way to achieve a functional device. For the most demanding device structures, layer thickness accuracies of better than 1% are often required.

Although a number of in-situ diagnostics for MBE growth are currently being developed, we feel that few have the potential for widespread adoption afforded by spectral reflectance. Those in general use today have rather severe limitations. RHEED oscillation measurement, which is by far the most commonly used technique with good accuracy, is generally only useful as a calibration prior to the growth of the actual device structure, and therefore is susceptible to short-to-moderate term drift or instabilities in growth rates. Much worse is the use of ionization gauges to measure flux, since these measurements are strongly affected by factors such as background pressure, temperature, and the history of gauge exposure to other species.

Of the developing techniques, optical sensors predominate. This is largely due to the good sensitivity of optical measurements, and to the possibility that these sensors may be located outside the relatively harsh environment of the deposition chamber. Spectroscopic ellipsometry (SE) is currently a contending technology. We believe, however, that SE as it is currently conceived is unnecessarily complex and sensitive for epitaxial growth monitoring. In fact, we feel that the extraordinary sensitivity of SE to factors such as surface and interface roughness are serious handicaps, as they lead to inordinately complex model fitting and computation. In addition, SE requires optical access to the growth surface at an angle which is not achievable in the vast majority of existing MBE machines. This angle must not vary by more than a few hundredths of a degree, effectively excluding the possibility of wafer rotation on typical MBE systems.

Spectral reflectance possesses a number of attributes which make it uniquely capable as a growth monitor. Because it is an optical technique and does not require the addition of components inside the growth chamber, it should be both stable and reliable. In contrast to SE, it uses normal incidence reflection, and thus should be insensitive to substrate rotation wobble and polarization effects. This means that the technique will be retrofittable on the majority of MBE systems in existence today. The sensitivity of the reflectance technique appears appropriate to a number of epitaxial device structures, and spectral interpretation will be only as complex as required for a reasonable determination of the epilayer parameters. Finally, this approach is appropriate for the construction of real-time control strategies for selected device structures.

CVD (Chemical Vapor Deposition) and MOCVD (Metal-Organic Chemical Vapor Deposition)

Chemical vapor deposition (CVD) is used to produce thin films by passing reactive gasses over a heated substrate. For compound semiconductor applications, metal-organic precursors such as trimethylgallium are used, hence the name MOCVD.

Unfortunately, CVD processing generally does not employ *in situ* sensors, and no method equivalent to RHEED is used routinely in CVD equipment today. This situation is likely to change in the near future as the high growth rate and multi-wafer capability of CVD is called upon to produce the complicated and exacting multiple-layer thin film structures required by the next generation of electronic and optoelectronic devices.

The fabrication of semiconductor thin films using (CVD) has traditionally been accomplished by introducing reactive gases into a chamber using timed sequences for a fixed set of reactor conditions. Temperatures, pressures, and flow rates are determined in advance by performing calibration runs before an actual device structure is produced. The results of these calibration runs are used in an iterative "dead reckoning" control strategy to make adjustments in the device structure recipe. Unfortunately, calibration runs must be performed whenever a new chemical source is added, equipment is replaced in the gas handling system, or a new device structure is to be grown. All reactors also experience drifts over time periods ranging from days to weeks, requiring re-calibration. Most calibrations are performed first with test structures and finally with repeated trials on the actual device structure using post-process *ex situ* analysis tools such as microscopy, photoluminescence, and X-ray diffraction methods. It is often very difficult to determine the origin of a failure or process deviation using post-growth analysis during the final fine tuning of the device structure recipe. The grower is often forced to guess what portion of the recipe needs alteration and then test this guess with another growth run. A large portion of the time and expense of thin film CVD is thus spent in calibration and post-process failure analysis.

Ideally, a thin film deposition system would utilize a sensor that determines the film thickness and composition at any instant in time. Such a sensor would allow one to easily implement feed-forward control and dispense with the currently used timed recipe or "dead reckoning" approach. Vigorous efforts are currently being made to develop such a sensor. As an interim step toward this goal, a simple method that can perform pre-growth calibrations and monitor deposition in real time would be an enormous improvement over current practices. Virtually all modern CVD equipment exhibits very stable behavior over the time period required to grow a thin film structure. The largest variations occur on a day-to-day basis, often involving some unexpected, discontinuous change in growth rate behavior. A RHEED-like tool for CVD applications would be a very effective way to measure and compensate for these variations, and may in fact provide all the control that is necessary for many device structures.

Approach

We present a simple and general method for extracting growth rates and optical constants from normal incidence reflectance obtained during the deposition of thin films. This method has been named ADVISOR for Analysis of Deposition using Virtual Interfaces and Spectroscopic Optical Reflectance. The method takes advantage of a "virtual interface" model to allow one to extract information from the topmost layer during the growth of a multiple-layer film structure. The technique is not subject to the cumulative errors that are encountered using multiple-layer models, and does not require precise knowledge of the positions of film interfaces. This method, combined with the simple and inexpensive equipment used to acquire the data, provides the equivalent of a RHEED tool for CVD applications. However, the reflectance tool is better than RHEED for real-time applications because it can monitor the growth of the film throughout the deposition process. RHEED is restricted to the first few monolayers of growth on nonrotating samples.

The method extracts growth rate and optical constant information from *in situ* measurements of normal incidence spectral reflectance during growth of a thin film. The growth may be on a substrate having any multiple-layer structure below the topmost film of interest. Normal incidence reflectance is chosen because it is simple, requires only one window for optical access, is insensitive to incidence angle in the near-normal direction, and is insensitive to light polarization. The latter two features provide several very practical advantages. Insensitivity to incidence angle allows one to monitor deposition on rotating (and therefore wobbling) substrates. Polarization insensitivity allows one to use inexpensive and stable broadband unpolarized light sources and optical relay systems such as multimode optical fibers that do not need to preserve polarization. The method does not require strain-free windows such as are necessary in ellipsometry or reflectance difference spectroscopy. Numerical analysis is also minimized at normal incidence because only *s* polarization need be considered, and the propagation angle inside the film does not need to be calculated.

ADVISOR is based on a model for thin film interference of coherent monochromatic light. In practice, the light need only have a wavelength bandwidth, $\Delta\lambda$, small enough to provide a coherence length, $\lambda^2/\Delta\lambda$, that is much longer than the optical thickness of the film, nd, where n is the index of refraction and d is the thickness of the film. A bandwidth of a few nanometers is sufficient to measure typical semiconductor films ($n \sim 4$) having a thickness of less than a few microns for 400 - 2000 nm light. Such bandwidths are readily obtained from a broadband source by using interference filters or short (1/4 or 1/8 m) focal-length spectrometers coupled with multi-element detectors.

The activities presented in this report can be viewed as an interim step between the traditional post-process analysis approach and real-time process control. With further development, real-time process control of thickness and composition using reflectance appears to be feasible. However, it is important to note that we have found the control strategy described in this paper to be completely adequate for growing even complex device structures such as vertical-cavity surface emitting lasers (VCSEL's). If the run-to-run behavior of the CVD reactor is sufficiently

stable over the time period of a few days, very little would be gained by attempting to adopt a real-time control strategy.

Description of the ADVISOR method

The Virtual Interface Concept

It is straightforward to model the reflectance from a smooth semiconductor substrate with an arbitrary number of smooth, homogeneous films deposited on it. The only parameters required are the complex refractive index for the substrate and the thickness and refractive index of each layer. If a growing film is monitored, reflectance interference oscillations are observed as the topmost film thickness changes with time. This time dependence is also straightforward to model by expressing the topmost film thickness as the product of a growth rate and the time.

There are, however, severe practical limitations that arise when such a straightforward approach is used to model the *in situ* reflectance wave form of a growing multiple-layer film. First, the deposition is performed at elevated temperatures. The optical constants of most semiconductor materials are not well known at the temperatures typical for CVD growth. This is particularly true for compound semiconductor alloys. Second, the thickness of a layer is not necessarily known precisely, particularly during a calibration run. In a multiple-layer reflectance model, errors in the refractive index and thickness of each layer contribute additively to uncertainties in the description of the growth of the topmost layer. This leads to a growth rate determination that is progressively less accurate with each additional calibration layer.

The solution to the multiple-layer reflectance modeling problem is to use a virtual interface concept, which is illustrated in Fig. 1. One chooses a virtual interface position (dashed line) that lies anywhere within the topmost film. It is then possible to rigorously describe the effects of all underlying layers as a single effective complex refractive index, N_{vi}, of a virtual interface effective substrate. The precise value of N_{vi} can, in principle, only be calculated from a complete knowledge of all the refractive indices and thicknesses of the underlying layers. However, if N_{vi} is taken to be an unknown, it is always true that any multiple-layer structure requires only two parameters, the real and imaginary parts of N_{vi}, to describe the effects of all underlying layers below the virtual interface boundary. Analysis of the topmost layer is thus made completely independent of the optical constants and interface positions of underlying layers. By choosing a new virtual interface position with each new layer, cumulative effects are eliminated in the analysis of a growing multiple-layer film structure. A full mathematical derivation and discussion of the theory behind this method is given in the Appendix of this report.

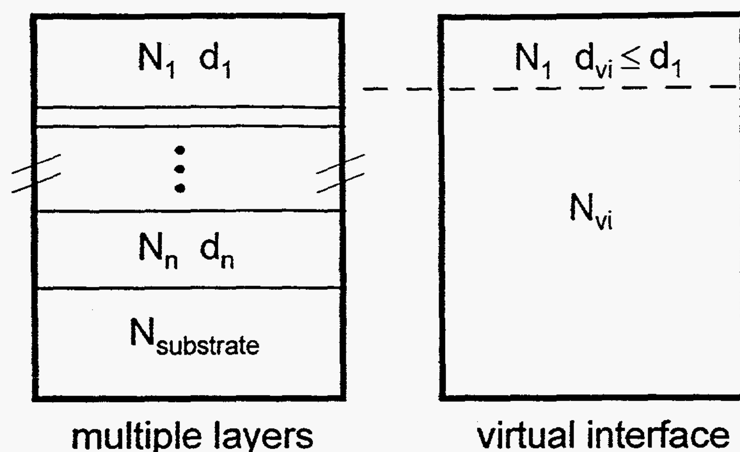

Fig. 1. Any multiple-layer thin film structure having refractive indices, N_i, and thicknesses, d_i, may always be modeled as a single-layer film on a virtual substrate with an effective refractive index, N_{vi}. All the optical effects of the various N_i and d_i are lumped into the value for N_{vi}. The virtual interface need not coincide with an actual interface, but must be somewhere inside the actual topmost film.

Growth Rate Extraction

The Appendix outlines a method by which one can use a reflectance waveform having several extrema of oscillations to estimate the values of the parameters to be fit. This becomes extremely useful for routine pre-growth calibrations. The calibration procedure is as follows: A multiple-layer film is grown and a single-wavelength *in situ* reflectance interferogram is recorded. Each layer is grown thick enough to provide several extrema of interference oscillations. The order of the layers and timing is chosen to yield good contrast between the interferograms in each layer. For example, a GaAs growth calibration layer is done after an AlAs calibration layer is placed on the GaAs substrate. Segments of data from each layer are chosen for analysis. The starting time for each segment is arbitrary, provided that it does not include the transition from one layer to the next. The choice of starting time changes only the value of r_{vi}, which is of no physical interest. Typically, the starting segment is chosen to be several seconds beyond the time at which the analyzed layer is known to have started. The stopping time is chosen to be a few seconds before the next layer is known to have started. The automated procedure outlined in the Appendix is used to provide starting estimates for the five-parameter fit. A least-squares analysis is then done to fit the data segment to the reflectance waveform and provide the growth rate for the layer. This can all be accomplished without prior knowledge about the growth rates or optical constants of the deposited materials. The process is then repeated for each layer in the calibration run. Fitting takes no more than a second for each layer.

The accuracy of G is related directly to the accuracy of the absolute reflectance. A one percent error in reflectance results in approximately a one percent error in growth rate. It is thus very important to self-calibrate the reflectance at the beginning of each run and to maintain instrument stability throughout the run.

RESULTS

Unfortunately, manufacturing defects in the MBE machine prevented us from implementing tests of real-time control. However, a pre-growth control strategy was developed on the EMCORE MOCVD reactor. This strategy led to an unprecedented demonstration of process control on one of the most difficult device structures that can be grown with compound semiconductor materials. Hundreds of vertical cavity surface emitting lasers (VCSEL's) were grown with only ± 0.3% deviations in the Fabry-Perot cavity wavelength – a nearly ten-fold improvement over current calibration methods. The success of this work has led to a great deal of interest from the commercial sector, including use of the ADVISOR method by Hewlett Packard and Honeywell. An improved reflectance design is to be submitted for a patent, and a small company, Pacific Lightwave, is incorporating the ADVISOR analysis method in its reflectometer product. Below are summaries of activities performed for the LDRD project.

Sensitivity Studies

Monte Carlo Simulations

Monte Carlo simulations were performed to explore the limits of accuracy of the ADVISOR method under ideal experimental conditions. Such studies are application specific, but serve to provide a general guide for what to expect from the technique. The case chosen was determination of the refractive index and the growth rate for an $Al_{0.25}Ga_{0.75}As$ film grown on GaAs. At 443 nm, a one percent error in the refractive index corresponds roughly to a one percent error in film composition. With ideal signal-to-noise (10^4), it is possible to obtain a one percent accuracy in the growth rate and composition with a film thickness on the order of $\lambda / 4n$. Accuracy improves exponentially with film thickness up to $\lambda / 2n$, at which point it becomes noise limited. These thicknesses may be excessive if one is considering real-time control of thin structures, but there is no such limitation on the thickness of a pre-growth calibration film.

If the refractive index is known beforehand and is not adjusted in the fit, 0.2% accuracy in the growth rate may be obtained after the first 10 nm of film growth. Even better accuracy is possible if the internal reflectance, r_i, is also known before the fit. In this case, 0.1% accuracy is achieved in the first 2 nm of film growth. Practical device structures that allow one to pre-determine parameters occur (or can be made to occur) in applications such as superlattices, quantum wells and high speed field effect transistor structures. These applications often have relatively thick underlying layers preceding a very thin layer whose thickness must be precisely

controlled. The non-critical lower layers may thus be used to advantage to facilitate convergence on critical layers.

Sensitivity Studies on HFET's and DBR (Distributed Bragg Reflectors)

Sensitivity studies have been performed on a target HFET structure. Originally we assumed that the HFET structure would contain InGaAs, but the final device chosen uses GaAs and two different compositions of AlGaAs, thus simplifying processing. The most difficult parameter to control in this device is threshold voltage, which is determined by both thin film layer thicknesses and doping densities. The reflectance method can only address layer thicknesses. Sensitivities ranging between 0.35 mV/Å and 1.85 mV/Å were found for the target HFET structure. This translates to 4.15 mV / % in the GaAs growth rate and 1.85 mV / % in the AlAs growth rate. Satisfactory control of threshold voltage variations via thickness may be obtained by controlling the growth rates to 1 % or better.

The sensitivity studies have shown that it should be possible to control thickness in both HFET and DBR applications in real time using an endpoint reflectance prediction based on ADVISOR determinations of growth rate and optical constants prior to the termination of the layer to be controlled. In the case of DBR mirrors, wavelengths shorter than the mirror stopband may be used to determine the growth rate with at least 0.1% accuracy because the quarterwave thickness is achieved earlier than that of the stopband. At elevated temperatures, the refractive index is larger than its room-temperature value, so this also contributes to obtaining an accuacte growth rate prior to the quarterwave thickness. Simulations show that it is always possible to find a critical wavelength such that the reflectance is changing rapidly just as the correct stack thickness is reached for each layer in the stack. Thus a simple reflectance endpoint scheme may be used to control DBR thickness of each layer, independent of previous layers. In a similar fashion, the thick AlGaAs buffer layer grown in an HFET application will allow us to accurately determine buffer optical constants and optical phases prior to the growth of the GaAs layer. Using the known optical constants of GaAs, only the growth rate needs to be determined while the i-channel, n-channel and spacer layers are deposited. An endpoint scheme may be used for precise determination of these layers. The 50% AlGaAs barrier layer is thick enough to be determined with the ADVISOR method, and the final GaAs cap may be treated in the same way as the channel layers.

ADVISOR Application to MBE growth

A single-wavelength reflectance probe was installed on the EPI MBE machine. Growth rates extracted with the ADVISOR method agreed within statistical deviations with growth rates obtained using conventional RHEED methods. Test structures were monitored during MBE growth, demonstrating an ability to detect even very thin features such as 100 angstrom superlattice structures. A plethora of installation problems with this new machine precluded further experiments with MBE applications.

ADVISOR Application to the Growth of VCSEL's

In this section, we illustrate the application of the ADVISOR method to the growth of an optoelectronic device structure. We choose the fabrication of a vertical cavity surface emitting laser (VCSEL) as an example of an extremely complex structure that requires many layers of differing alloy composition and very precise thickness control. The strategies used in this structure provide a general example of how the method may be implemented in other applications.

Apparatus

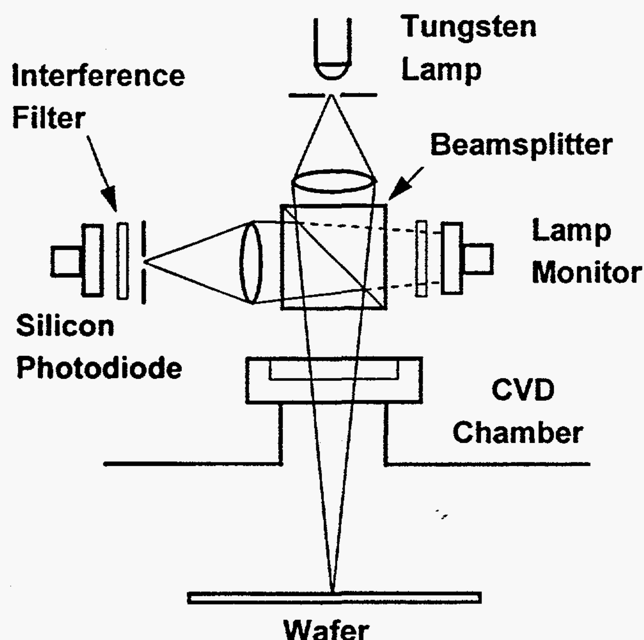

Fig. 2. Schematic of the instrument used to record normal incidence reflectance. A 633 nm interference filter was used for all the data.

The apparatus is shown in Fig. 2. It is a non-intrusive, compact assembly, measuring only 15 cm in its longest dimension, that mounts directly on the top window of the reactor. A 7 watt tungsten halogen lamp is used for the light source. This lamp is chosen because it is small, inexpensive, more stable in amplitude than most lasers, and provides a continuous range of wavelengths from 350 nm to several microns. The lamp illuminates a 0.5 mm aperture which is imaged as a 2.5 mm spot on the wafer using a 15 mm diam., 50 mm focal length lens. The light is directed through a 3/4 in. diam. purged window above the wafer carrier in a commercial EMCORE 3200 rotating disk CVD reactor. Reflected light is deflected with a beam splitter, imaged on a 0.6 mm aperture, and detected with a silicon photodiode placed behind a 10 nm bandwidth interference filter. The current from the photodiode is fed to a transimpedance amplifier and the output is digitized with an A/D board in a personal computer. A monitor

photodiode with an identical interference filter is also mounted on the beam splitter. The reflected light signal is divided by the monitor signal to cancel out fluctuations and drifts in the lamp source. Window and interference filter surfaces must be tilted slightly to eliminate spurious reflections. Spectral reflectance may be implemented with this apparatus by replacing the 0.6 mm aperture with a 0.6 mm optical fiber connected to a spectrograph.

The optical arrangement in Fig. 2 serves several purposes. 1) It provides a means by which a relatively small spot of light may be imaged on the surface of the substrate using a highly divergent lamp source. 2) It relays the image of the first aperture to the surface of the wafer and then to the receiving aperture. The spot on the substrate thus acts as an effective source for the second lens. Due to the conjugate relationship between the spot on the substrate and the receiving aperture, small shifts in the position and tilt of the substrate do not significantly affect the flux of light passing through the receiving aperture. 3) It acts both as a spatial filter as well as a wavelength filter. Light originating from the much brighter 3000 K lamp source completely overwhelms the ~1000 K thermal radiation from the spot on the heated substrate viewed by the receiving aperture. This allows one to directly record the DC signal without chopping or lock-in detection. Current to voltage conversion with the transimpedance amplifier is performed in a photovoltaic mode without reverse bias on the silicon photodiode. This provides a linear signal with a drift-free, true-zero baseline and negligible dark current.

Absolute reflectance is obtained by referencing the starting signal to the known reflectance of the substrate before deposition begins. This provides a self-calibration at the beginning of each growth run.

GaAs and $Al_xGa_{1-x}As$ layers were typically grown at 750 °C by using trimethylaluminium (TMA), trimethylgallium (TMG), and 100% arsine (AsH_3). The alkyl sources carried by high-purity H_2 were injected into the reactor through 3 different injection zones distributed along the radial direction of the top flange. The gas-flow partitioning for alkyl sources among these three injection zones was set at 7%:78%:15% between the inner, middle, and outer zones to give the best thickness uniformity across the wafer. The substrate was rotated at 1000 rpm at a pressure of 60 torr. Group V flow and total reactor flow were 248.5 sccm and 32.6 slm, respectively.

Thin Film requirements for VCSEL Growth

Our VCSEL device consists of over 600 layers of $Al_xGa_{1-x}As$ alloys. The composition, x, of the alloy is piece-wise linearly graded to emulate a parabolic composition profile in the layers that comprise the distributed Bragg reflector (DBR) stacks. The bottom mirror stack is doped n-type and the top stack is doped p-type. The n-type doping poses no problems, but p-type doping is achieved using CCl_4 as a source gas. The chlorine in this source causes an etchback reaction to occur that alters the overall deposition rate of the doped $Al_xGa_{1-x}As$ alloy. The etchback rate is a function of alloy composition and growth temperature, which complicates the growth of the graded alloy layers. Two deposition temperatures are required for successful device performance. Because the cavity region of the device may require very different growth rates than the DBR stacks, two sources of Ga and two sources of Al are necessary to avoid pauses in

the growth recipe. Calibration of such a complicated structure is formidable using traditional post-process calibration methods.

After some preliminary reflectance experiments to investigate the growth behavior of the system, it was determined that a VCSEL structure could be calibrated with a single run. Below is a summary of the preliminary experiments, followed by a description of the final calibration procedure.

General AlAs and GaAs Growth Behavior

A growth run was performed to determine the overall behavior of the reactor during the deposition of AlAs and GaAs. The reflectance waveform from this run is shown in Fig. 3. Alternating layers of AlAs and GaAs were grown at 750 °C, each layer having a different source gas flow rate. The different growth rates that result from this experiment are readily apparent as different oscillation frequencies. Fig. 4 shows the virtual interface analysis of the data in Fig. 3. Each data point represents a virtual interface analysis from one segment of data in Fig. 3. The growth rates are seen to be linear in source gas flow rate, as would be expected in a diffusion-limited CVD reaction. The composition, x, of $Al_xGa_{1-x}As$ alloys is linearly related to the relative growth rates of AlAs and GaAs. These two linear features greatly simplify the task of growing a VCSEL structure in which the DBR stacks must be graded in composition. A complete calibration requires only the determination of the growth rate of AlAs and GaAs at one flow rate. This measurement is sufficient to determine the slopes of the lines in Fig 4. From this, one may calculate all necessary flow rates for a series of graded-composition $Al_xGa_{1-x}As$ alloy layers.

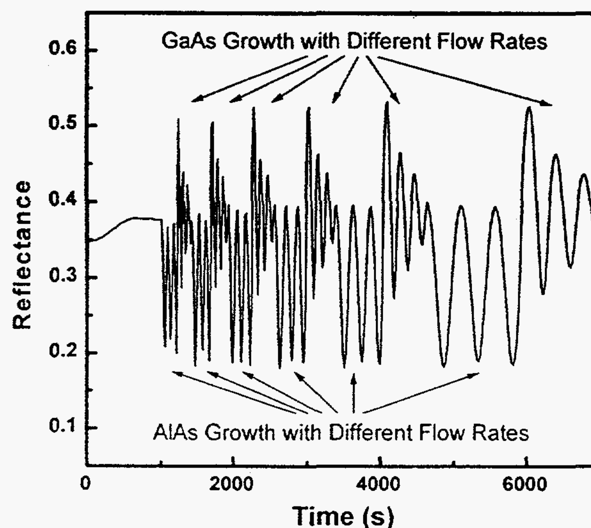

Fig. 3. Reflectance from twelve layers of alternating AlAs(2500 Å)/GaAs(2500 Å) thin films. Different alkyl flow rates were used for each layer.

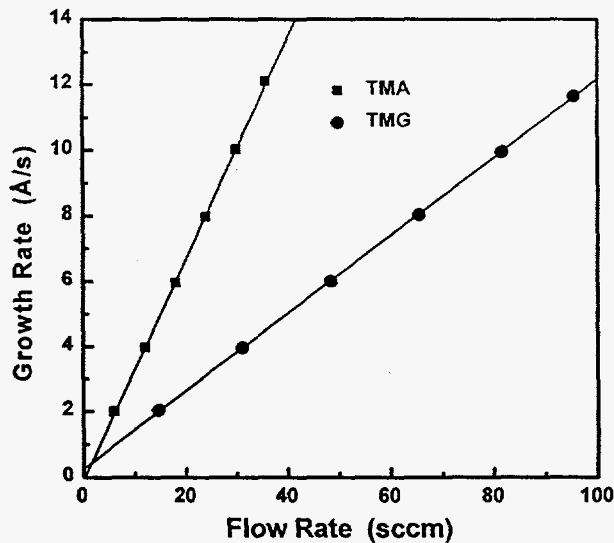

Fig. 4. Growth rates as a function of alkyl flow rate extracted from the data in Fig. 3 using virtual interface analysis.

Fig. 4 also reveals that the TMG flow controller has a small but significant zero offset. A high-precision tool such as the reflectance probe is needed to reveal this kind of deviation.

Etchback Growth Behavior

A calibration run similar to that of Fig. 3 was performed for a range of alloy compositions, with and without doping. From the virtual interface analysis of the growth rates, calibration functions were constructed to allow one to compensate for etchback effects at any composition. As with the general calibration above, it was determined that only one etchback measurement was needed to completely determine the flow rates required to produce p-type DBR's.

Specific Calibration Scheme for 845 nm and 770 nm VCSEL's

After the background work outlined above, it was determined that a single calibration run involving only six layers is necessary to completely characterize the system for growth of a VCSEL centered at either 845 nm or 770 nm. The reflectance interferogram from such a calibration is shown in Fig. 5. The run determines the 750 °C growth rates from the first Al source, the first Ga source, the second Al source, the second Ga source, and the etchback rate when CCl_4 is introduced. Finally, the temperature is dropped to 640 °C and another growth rate with CCl_4 doping is determined. In a single run lasting less than one hour, all calibration information is obtained with the *in situ* reflectance monitor.

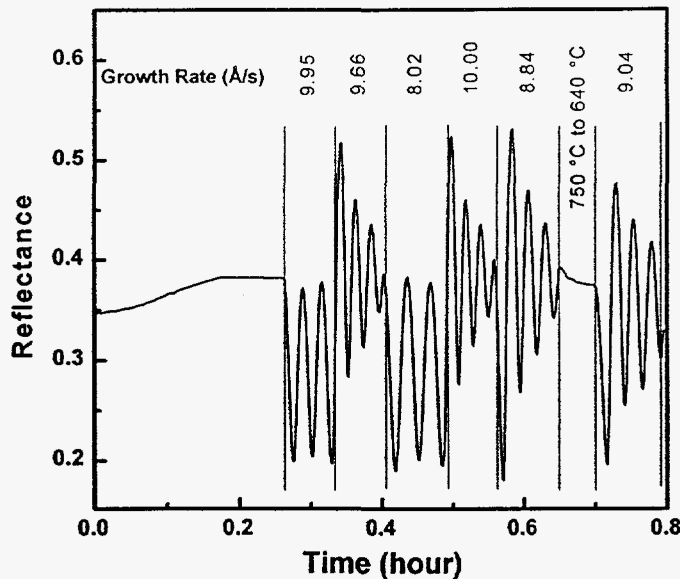

Fig. 5. Reflectance interferogram for a six-layer pre-growth calibration run. All information needed to set up a growth recipe for a VCSEL is obtained from this calibration run.

The above calibration scheme yields working VCSEL devices without the need for further fine tuning of the system. Because our CVD reactor is very reproducible, only periodic re-calibration is needed between a series of runs. Fig. 6 shows the results of many VCSEL growths in which the calibration was performed only before each group of runs shown. A good figure of merit for VCSEL's is the reproducibility of the Fabry-Perot cavity wavelength. Excellent reproducibility is obtained, and the target wavelength is achieved with the first device grown after each calibration. Also note that a single 845 nm run was inserted within the group of 770 nm VCSEL's. Calibration values from the 770 nm group were used to compute the recipe for the single 845 nm run. This represents a good example of the agile manufacturing capability of the pre-calibration method.

Real Time Growth Monitor

In addition to its use as a calibration tool, the reflectance instrument is used to monitor the growth of every structure. Fig. 7 shows a typical reflectance interferogram of an 845 nm VCSEL run. It is easy to observe the growth of the buffer layer, *n*-type DBR, laser cavity region, *p*-type DBR, and the contact cap layer. Such a monitor is extremely valuable as a real time fault detector, signaling such events as a depleted source or a rough surface. In addition to detecting the presence of a fault, the reflectance history can very often pinpoint the source of the failure. This eliminates the need to perform additional diagnostic growth runs to track down and identify what actually caused the failure.

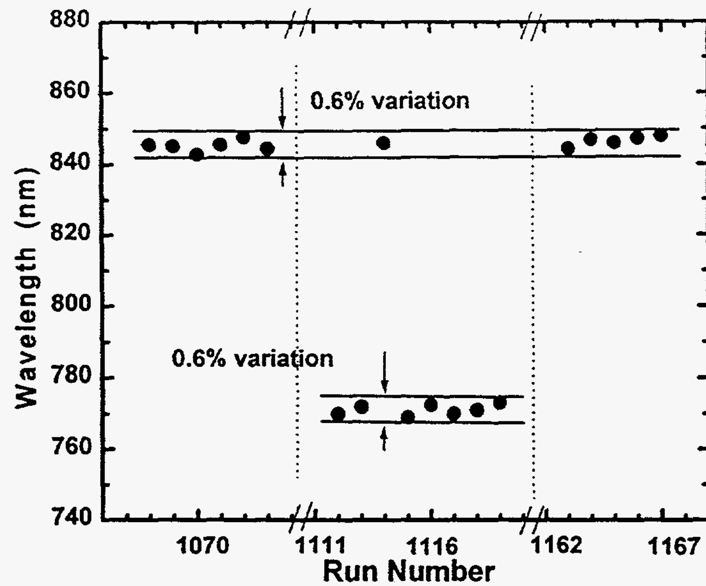

Fig. 6. Reproducibility of the cavity wavelength of 770 nm and 845 nm VCSEL structures. A virtual interface calibration was performed before each group of data shown.

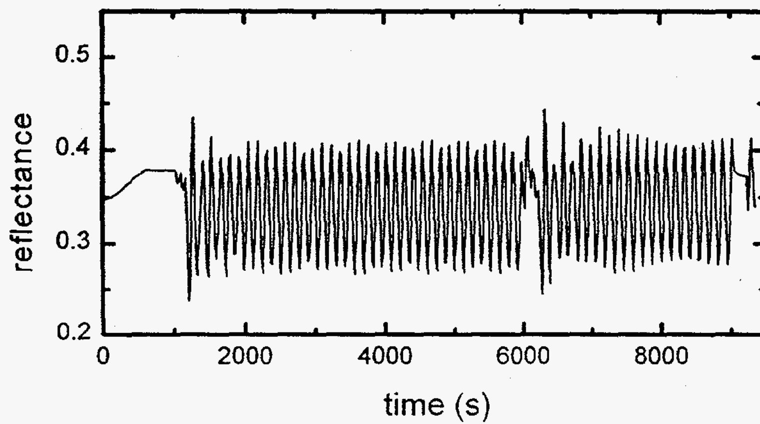

Fig. 7. A reflectance interferogram recorded during the complete growth of a 845 nm VCSEL.

SUMMARY

This project has exceeded our expectations. Although equipment limitations prevented us from achieving all of our second-year goals in this project, it is clear that *in situ* reflectance has made a major impact on thin-film processing control and almost assuredly will change the way that compound semiconductor devices are made in the future. We have obtained *in situ* spectral reflectance data with 2×10^{-4} RMS noise and have measured growth rates with a precision of at least 0.3%. A new method: Analysis of Deposition with Virtual Interfaces and Spectroscopic Optical Reflectance (ADVISOR) has been developed for extracting growth rates and optical constants from the topmost layer of a growing film. This method eliminates cumulative errors that arise from multiple layer models and also eliminates the need for precise knowledge of high temperature optical constants and interface boundary positions of all layers in a complex structure. Sensitivity studies have been performed for 1) the ADVISOR method, 2) HFET test structures and 3) VCSEL structures. Straightforward schemes using reflectance endpoint prediction have been proposed for real time thickness control of HFETs and the distributed Bragg reflectors (DBR) in a VCSEL structure. A single wavelength prototype reflectance instrument installed on a commercial EMCORE reactor has quickly become a workhorse tool for pre-growth calibration. This strategy led to an unprecedented demonstration of process control on one of the most difficult device structures that can be grown with compound semiconductor materials. Hundreds of vertical cavity surface emitting lasers (VCSEL's) were grown with only ± 0.3% deviations in the Fabry-Perot cavity wavelength — a nearly ten-fold improvement over current calibration methods. The success of this work has led to a great deal of interest from the commercial sector, including use of the ADVISOR method by Hewlett Packard and Honeywell. An improved reflectance design is to be submitted for a patent, and a small company, Pacific Lightwave, is incorporating the ADVISOR analysis method in its reflectometer product.

PUBLICATIONS

The work in this report has led to the following publications:

1. W. G. Breiland and K. P. Killeen, "A virtual interface method for extracting growth rates and high temperature optical constants from thin semiconductor films using *in situ* normal incidence reflectance", J. Appl. Phys. 78 (1995) 6726.
2. W. G. Breiland, T. M. Brennan, H. C. Chui, B. E. Hammons, and K. P. Killeen, "Normal Incidence Reflectance: A Robust Tool for In Situ Real-Time Measurement of Growth Rates and Optical Constants of CVD-Grown Semiconductor Thin Films", Proceedings of the Symposium on Process Control, Diagnostics, and Modeling in Semiconductor Manufacturing, M. Meyyappan, D. J. Economou, and S. W. Butler, eds., The Electrochemical Society, Inc, Proceed. Vol 95-2, 1995, pp 261-269.
3. W. G. Breiland, H. Q. Hou, H. C. Chui, and B. E. Hammons, "In Situ Pre-Growth Calibration Using Reflectance as a Control Strategy for MOCVD Fabrication of Device Structures", To be published, J. Crystal Growth, 173 (1997) xxx.

4. W. G. Breiland, H. Q. Hou, B. E. Hammons, and S. A. Chalmers (Pacific Lightwave), "In Situ Spectroscopic Reflectance and Virtual Interface Analysis of MOCVD-grown $Al_xGa_{1-x}As$ Alloys", To be published, J. Electron. Mat., 1997.

Appendix: Thin film reflectance physics and the ADVISOR method

Maxwell equations at an interface

We start with a flat interface between two homogeneous, isotropic, semi-infinite slabs of material having complex refractive indexes, N_1 and N_2. We assume that reflected and refracted light is described in terms of inhomogeneous electromagnetic (EM) waves with the following phase convention for the electric field vector, $\vec{E}$:

$$\vec{E} = \vec{A}e^{i(\omega t - \vec{\kappa}\bullet\vec{r})} \qquad \text{A1.}$$

The wavevector, $\vec{\kappa} = \vec{u}2\pi N / \lambda$, is defined in terms of a *complex* unit propagation vector, $\vec{u}$, the complex refractive index, $N = n - ik$, and the vacuum wavelength, λ. Reflectance is determined from ratios of the complex electric field amplitudes, $\vec{A}$, of forward and backward propagating waves. With the benefit of hindsight, a coordinate system is chosen with an incident inhomogeneous wave propagating in the *x-y* plane, traveling in the +*x*, +*y* direction, originating in medium 1. The interface is placed in the *y-z* plane:

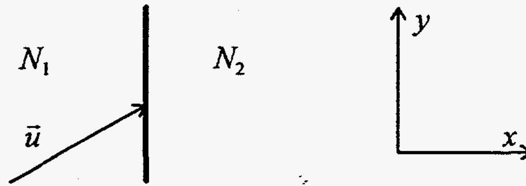

Application of boundary conditions for the interface yields, from Maxwell's equations, the following results:

1) The frequency, ω, is unchanged in passing through the boundary. When ratios of electric fields are taken, the time dependence cancels out, leaving only spatially varying electric fields to consider.

2) The incident EM wave is split into only two distinct waves at the interface: a transmitted (refracted) forward-propagating wave that passes into medium 2, and a reflected backward-propagating wave that stays in medium 1. The propagation vectors of reflected and refracted waves are confined to a plane, termed the "plane of incidence", that is defined by $\vec{u}_1$ and the vector normal of the material interface plane. The above coordinate choice places the plane of incidence in the *x-y* plane, implying that $\vec{u}_1$ has only *x* and *y* components.

3) In addition to the EM waves discussed above, Maxwell's equations allow only one additional possibility: a complimentary wave originating in medium 2 and propagating in the backward direction may also exist at the interface. This wave represents a reflected EM field

from some other parallel interface to the right. Thus, the general case yields four possible EM waves at each interface in a multilayer film with the following spatial relationships:

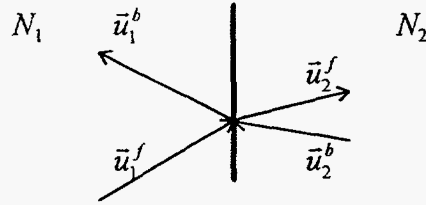

The symbols *f* and *b* indicate "forward" and "backward" propagating waves, respectively.

4) Two independent polarization directions for each electric field vector are supported by the wave/interface combination. An EM wave with the electric field parallel to the plane of incidence is referred to as "p" polarized light (also called TM for transverse magnetic), and a wave with the electric field perpendicular to the plane is "s" polarized (also called TE for transverse electric). The "s" comes from the German word for perpendicular.

5) The *y* component of $\vec{\kappa}$ is unchanged in passing through the boundary (Snell's law), $\kappa_{1y} = \kappa_{2y}$, or $N_1 u_{1y} = N_2 u_{2y}$. Looking ahead to applications beyond a simple interface, this result gives the following useful relationships: A plane wave in a non-absorbing medium with refractive index N_0 incident at an angle θ on an *n*-layer stack has $u_{0y} = \sin\theta$. From Snell's law, therefore, all materials in the stack obey:

$$N_0 \sin\theta = N_1 u_{1y} = N_2 u_{2y} = \ldots = N_n u_{ny} \qquad \text{A2}$$

This gives a value for the *y* component of $\vec{u}$ for any material in the stack in terms of its refractive index and the incident-wave product $N_0 \sin\theta$. Moreover, $\vec{u}$ is a unit vector, $u_x^2 + u_y^2 = 1$, so the *x* components of $\vec{u}$ may be obtained directly from the *y* components of $\vec{u}$, $u_{mx} = \sqrt{1 - u_{my}^2}$. In general, the components of $\vec{u}$ are complex numbers.

6) The boundary conditions lead to relationships between the amplitudes of the forward, A^f and backward, A^b, propagating waves in each medium, 1 or 2, at the interface. These are most conveniently expressed in terms of matrix relations for each polarization:

$$\begin{bmatrix} A_1^f \\ A_1^b \end{bmatrix}_s = \frac{1}{2N_1 u_{1x}} \begin{bmatrix} N_1 u_{1x} + N_2 u_{2x} & N_1 u_{1x} - N_2 u_{2x} \\ N_1 u_{1x} - N_2 u_{2x} & N_1 u_{1x} + N_2 u_{2x} \end{bmatrix} \begin{bmatrix} A_2^f \\ A_2^b \end{bmatrix}_s \qquad \text{A3}$$

$$\begin{bmatrix} A_1^f \\ A_1^b \end{bmatrix}_p = \frac{1}{2N_1 u_{1x}} \begin{bmatrix} N_2 u_{1x} + N_1 u_{2x} & N_2 u_{1x} - N_1 u_{2x} \\ N_2 u_{1x} - N_1 u_{2x} & N_2 u_{1x} + N_1 u_{2x} \end{bmatrix} \begin{bmatrix} A_2^f \\ A_2^b \end{bmatrix}_p \qquad \text{A4}$$

The above expressions describe the general case for all possible EM fields that can exist at the interfaces of multiple-layer stacks of isotropic, homogeneous, materials. It includes the possibility that there may be an electric field amplitude from a backward propagating beam in medium 2, resulting, for example, from a reflection from some other parallel interface to the right. The reflection coefficient, r_{12}, is defined to be the ratio of backward to forward wave amplitudes in medium 1 at the interface, $r_{12} = A_1^b / A_1^f$. If medium 2 is a semi-infinite slab with no other interfaces to the right, then the amplitude A_2^b is known to be zero. This yields relatively simple expressions for the s and p reflection coefficients:

$$r_{12}^s = \left(N_1 u_{1x} - N_2 u_{2x}\right) / \left(N_1 u_{1x} + N_2 u_{2x}\right) \qquad \text{A5}$$

$$r_{12}^p = \left(N_2 u_{1x} - N_1 u_{2x}\right) / \left(N_2 u_{1x} + N_1 u_{2x}\right) \qquad \text{A6}$$

If the formal definition, $u_{ix} = \cos\theta_i$, is used ($\cos\theta_i$ is possibly complex), then the above expressions for r_{12} yields the standard expressions for the "Fresnel coefficients" quoted in optics textbooks.

The general expression for an interface in the 2×2 matrix formalism may be re-written as:

$$C\begin{bmatrix} A_1^f \\ A_1^b \end{bmatrix} = \begin{bmatrix} 1 & r_{12} \\ r_{12} & 1 \end{bmatrix} \begin{bmatrix} A_2^f \\ A_2^b \end{bmatrix} \qquad \text{A7}$$

The factor C will always cancel out when the ratio of electric field amplitudes is used to calculate the reflection coefficient. The above 2×2 matrix is called the "interface matrix", I_{12}. Note that the order of subscripts is important. By convention, the left index denotes the medium closest to the incident wave.

The above expression completely defines the relative relationships between wave amplitudes at an interface. Inside any material, the forward and backward inhomogeneous EM waves propagate independently of each other with a spatial phase factor, $\kappa_x x$. If the origin for x is chosen to be at an interface, then a matrix expression may be constructed that relates the electric field amplitudes at a position x with the amplitudes at the interface:

$$\begin{bmatrix} A^f \\ A^b \end{bmatrix}_x = \begin{bmatrix} \exp(+i2\pi Nx/\lambda) & 0 \\ 0 & \exp(-i2\pi Nx/\lambda) \end{bmatrix} \begin{bmatrix} A^f \\ A^b \end{bmatrix}_{x=0} \qquad \text{A8}$$

Convention dictates that the thickness of a film, x, is measured from an interface on the right, and proceeds to the left, in the $-x$ direction, leading to the signs for the exponents in the above formula. This convention allows one to start with a semi-infinite substrate on the right, building thin-film layers toward the incident wave. The above 2×2 matrix is referred to as a "layer matrix", L. In the spirit of eliminating as may common factors as possible in the matrix expressions, an alternative form may be used for the layer matrix:

$$L \equiv \begin{bmatrix} 1 & 0 \\ 0 & Z \end{bmatrix}, \quad Z \equiv \exp(-i4\pi Nx / \lambda) \qquad \text{A9}$$

General Expression for Multiple-layer Thin Film Reflectance

The relative amplitudes of the electric field at the surface of a multiple-layer film may be determined by starting inside the semi-infinite substrate where it is known that A^b is zero. A series of interface and layer matrices may then be constructed, yielding an expression for the amplitudes at the surface of the multilayer stack in terms of the amplitudes inside the substrate. Dividing through by $A^f_{substrate}$, an equation is obtained whose RHS is completely determined. For an *n*-layer film,

$$C\begin{bmatrix} A^f \\ A^b \end{bmatrix}_{surface} = I_{01}L_1I_{12}L_2 \ldots I_{n-1,n}L_nI_{n,substrate}\begin{bmatrix} 1 \\ 0 \end{bmatrix}_{substrate} \qquad \text{A10}$$

Formally, the reflection coefficient is obtained by performing the matrix products indicated in the above expression and taking the ratio of the resulting vector elements, $r = A^b / A^f$. The observed reflectance is $R = |r|^2$.

Virtual interface model

We focus our attention on simultaneously extracting *both* the optical constants *and* the growth rate of a film because this is what is often expected from a pre-growth calibration tool. This is particularly true for compound semiconductor films where both chemical composition and growth rate need to be determined. We assume that each layer to be analyzed is a homogeneous, isotropic, flat film of infinite extent in the plane normal to the direction of incidence. Each layer is characterized by a single complex refractive index, $N = n - ik$, that does not vary within the layer. The refractive index may be a function of other physical parameters such as temperature, wavelength, and chemical composition. We assume that all such variables are held fixed during the growth of the analyzed layer. We also assume that the growth rate of each layer is constant in time.

With the above assumptions, the normal incidence optical behavior of an n-layer film is given by equation A10 in the equivalent form:

$$\begin{bmatrix} A_f \\ A_b \end{bmatrix}_{\text{surface}} = I_{01}L_1I_{12}L_2 \ldots I_{n-1,n}L_n\begin{bmatrix} A_f' \\ A_b' \end{bmatrix}_{\text{substrate}}. \qquad \text{A11}$$

The nth-layer/substrate interface matrix, $I_{n,substrate}$, has been multiplied with the substrate electric field amplitude vector. The primed terms are the electric field amplitudes just *inside* the nth layer at the interface with the substrate. Neither of these amplitudes is zero, in general. We retain the substrate notation on the primed field vector because it is still located at the substrate interface boundary.

The virtual substrate model is obtained trivially from Eq. A11 by noting that all matrix multiplication from I_{12} to the substrate electric field vector may be performed, yielding a new equation that looks identical in form to Eq. A11 for a single-layer film:

$$\begin{bmatrix} A_f \\ A_b \end{bmatrix}_{\text{surface}} = I_{01} L_1 \begin{bmatrix} A_f'' \\ A_b'' \end{bmatrix}_{\text{vs}} . \qquad \text{A12}$$

The double-primed electric field amplitudes, which formally are the result of (possibly many) matrix multiplications, may be considered to be the result of a single interface and one virtual semi-infinite substrate, as implied by the "vs" subscript. Note that the virtual substrate is nothing more than a conceptualization, not an approximation, because it is derived directly from the rigorous n-layer expression, Eq. A11. Equation A12 states that each new layer in a growing multiple-layer film may rigorously be thought of as a simple single layer on a virtual substrate.

A further observation that is very important for the practical implementation of the virtual substrate model is derived from the expression for the layer matrix, Eq. A9. This matrix may be factored into the product of two diagonal matrices in which the layer thickness, d, is split into two parts: $d-x$, and x. The rightmost matrix may then be multiplied by the electric field amplitude vector, again yielding a single-layer virtual substrate form with layer thickness $d-x$. Thus, even a portion of the topmost layer may itself be considered to be part of the virtual substrate. The term, "virtual interface" is used to describe this choice of virtual substrate. As will be demonstrated below, the virtual interface approach allows one to extract growth rates and optical constants without having to know the precise location or nature of any interfaces, and can yield meaningful information on a film that is mostly homogeneous, except perhaps for a small region in the vicinity of the real interface.

The complex reflectance is defined to be the backward-propagating electric field amplitude divided by the forward amplitude. Eq A12 yields

$$r(t) = \frac{r_\infty + r_i \exp(-i4\pi NGt/\lambda)}{1 + r_\infty r_i \exp(-i4\pi NGt/\lambda)}, \qquad \text{A13}$$

where the subscript, 1, has been dropped from the refractive index. The film thickness has been re-expressed as the growth rate, G, times the time, t ,where the virtual substrate interface is defined to be the position of the growth front at $t = 0$. r_∞ is the complex reflectance of an infinitely thick film of the topmost layer and is given explicitly by $(1-N)/(1+N)$. r_i is the

complex reflectance just inside the layer ("internal layer reflectance") and is the ratio of backward and forward electric field amplitudes, $A_b^{''}/A_f^{''}$, at the virtual substrate interface, Eq. A13. It is not an observable reflectance because it exists within the topmost layer, but its value may be inferred from the observable reflectance as demonstrated below.

The value of the internal reflectance and the film optical constants may be used to formally define a virtual substrate refractive index, N_S, with the expression: $r_i = (N - N_s)/(N + N_s)$. N_S has no physical significance except in the case of a single-layer film on an actual homogeneous substrate, but it is sometimes useful to relate r_i to N_S in order to understand the behavior of an observed reflectance waveform.

The observable real reflectance, $R = |r|^2$, is given by:

$$R(t) = \frac{R_\infty - 2\sqrt{R_\infty R_i}\, e^{-\gamma t}\cos(\delta t - \sigma - \varphi) + R_i e^{-2\gamma t}}{1 - 2\sqrt{R_\infty R_i}\, e^{-\gamma t}\cos(\delta t - \sigma + \varphi) + R_\infty R_i e^{-2\gamma t}} \quad . \qquad \text{A14}$$

The following definitions are used in Eq. A14:

$$R_\infty = |r_\infty|^2 = \frac{(1-n)^2 + k^2}{(1+n)^2 + k^2}$$

$$\varphi = \tan^{-1}\left(\frac{2k}{n^2 + k^2 - 1}\right)$$

$$R_i = |r_i|^2 = \left|\sqrt{R_i}\, e^{i\sigma}\right|^2 = \frac{(n - n_s)^2 + (k - k_s)^2}{(n + n_s)^2 + (k + k_s)^2} \qquad \text{A15}$$

$$\sigma = \tan^{-1}\left(\frac{2(nk_s - n_s k)}{n^2 - n_s^2 + k^2 - k_s^2}\right)$$

$$\gamma = 4\pi kG/\lambda$$

$$\delta = 4\pi nG/\lambda$$

Expressions involving virtual substrate optical constants have been included in Eq. A15 to show the connection between an actual substrate and the above quantities.

Equation A14 is an exact expression (within the confines of our earlier assumptions) for the observed normal incidence reflectance of a film growing on top of an arbitrarily complicated multiple-layer substrate. *R(t)* is completely determined by five parameters: *n, k, G,* R_i, and σ. The first three are parameters of physical interest; the last two define the cumulative optical response of all the underlying layers, but may simply be treated as fitting constants for the purposes of obtaining the first three parameters. Because reflectance yields only one value per measurement, at least five reflectance measurements at five different times are necessary to

determine n, k, and G at a given wavelength. $R(t)$ may be monitored throughout the growth process; n, k, and G may thus be determined for each layer in a multiple-layer structure before they effectively become lumped into R_i and σ.

The following observations can be made about Eq. A14: (1) $R(t)$ contains terms that are oscillatory with a frequency that depends only on the factor nG/λ. (2) The periodic terms of $R(t)$ are damped with exponential terms that depend only on the factor kG/λ. The shapes of $R(t)$ range from almost purely sinusoidal oscillations to non-sinusoidal shaped curves with alternating rounded and cusp-like extrema. (3) The virtual substrate manifests itself in two features of the oscillatory waveform. The amplitude of the internal complex reflectance, $|r_i|$, determines in part the amplitude of the oscillatory waveform and is therefore directly manifested as the contrast between $R(t > 0)$ of the film and previous R values of the virtual substrate. The phase of the internal complex reflectance, σ, appears as a fixed phase-shift term in the cosine expression. It may take on any value between $-\pi$ and π, depending on the relative magnitudes of the virtual substrate optical constants and the choice of $t = 0$. Note that there are no time-dependent terms in Eq. A15 that contain R_i or σ, stemming from the fact that r_i is fixed at $t = 0$ and does not change as the film grows. All time-dependent reflectance behavior for $t > 0$ is due strictly to n, k, and G.

Extraction of growth rate and optical constants: The ADVISOR method

Further insight into Eq. A14 may be obtained with an approximation that is often valid for semiconductors. Referring to the expression for R_i in terms of the virtual substrate optical constants in Eq. A15, we note that R_i can be $<< 1$ if the film and substrate both have high refractive indexes (~4) and they are not too different from each other. In addition, The phase shift term, φ, becomes negligible for weakly absorbing films, where $k << 1$. Under these two conditions, Eq. A14 becomes the much simpler damped cosine expression:

$$R(t) \cong R_\infty - 2\sqrt{R_\infty R_i}(1 - R_\infty)e^{-\gamma t}\cos(\delta t - \sigma). \qquad \text{A16}$$

This expression is the starting point for a simple method for extracting the growth rate and optical constants from $R(t)$. Each of the physical parameters of interest is directly manifested as a distinct characteristic in the reflectance waveform. If a film is grown sufficiently thick to provide at least three reflectance extrema, reasonable starting estimates for all five parameters may be made with an automated algorithm that requires no *a priori* knowledge of the values of the parameters.

Figure A1 illustrates a typical reflectance waveform and the information that is required to provide estimates of n, k, G, R_i and σ. The waveform oscillates and damps symmetrically to R_∞ at long times. An estimate of R_∞ is therefore obtained from the mean value of the oscillating waveform over time. The frequency, δ, is obtained from the half-period, T, of the oscillation at

the crossing points with R_∞. The decay constant, γ, is obtained from an exponential fit to the decay of two extrema, R_m and R_{nm}, on the same side of R_∞ and separated in time by T_m. Estimates for σ and R_i may be obtained from the reflectance and its time derivative at $t = 0$. (Alternatively, σ may be estimated from the time between $t = 0$ and the first positive-slope R_∞ crossing.)

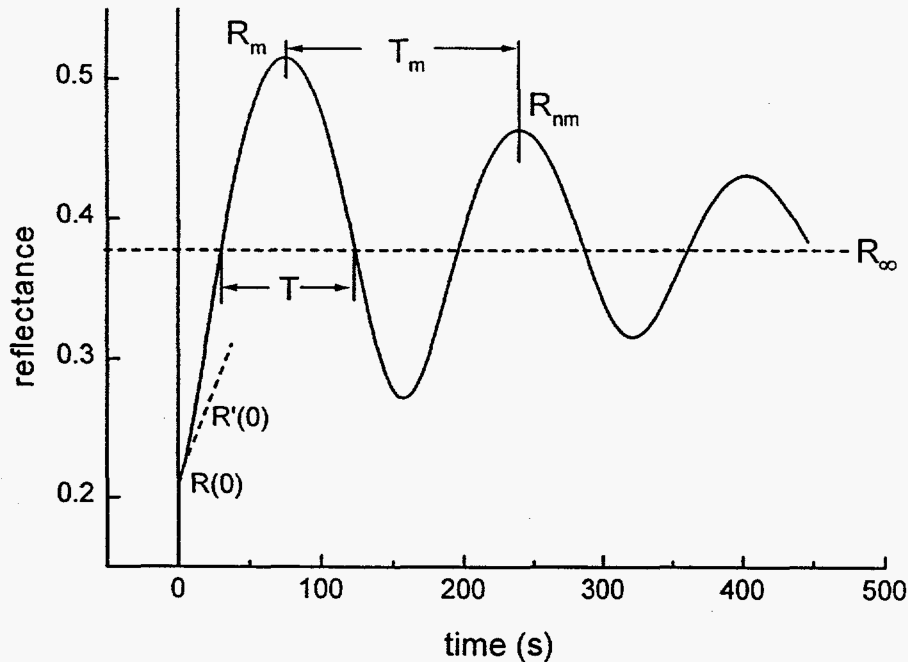

FIG. A1. Quantities that may be obtained from a typical reflectance *vs* time interference waveform to provide estimates for a least squares fit to Eq. A14. Each of the parameters, n, k, G, R_i, and σ is responsible for a distinct characteristic feature in the waveform. nG determines the frequency, kG the damping, σ the phase shift, and R_i the amplitude.

The above values allow one to solve for the desired five parameters with the following expressions:

$$
\begin{aligned}
&R_\infty \cong \langle R(t) \rangle_t \\
&\delta \cong \pi / T \\
&\gamma \cong \ln\left(R_m / R_{nm}\right) / T_m \\
&G \cong \frac{\lambda\delta}{4\pi}\left[\frac{1+R_\infty}{1-R_\infty} - \sqrt{\left(\frac{1+R_\infty}{1-R_\infty}\right)^2 - \frac{\gamma^2+\delta^2}{\delta^2}}\right] \\
&n \cong \lambda\delta / 4\pi G \\
&k \cong \lambda\gamma / 4\pi G \\
&\sigma \cong \tan^{-1}\left(\frac{-R'(0)/\delta}{R_\infty - R(0)}\right) \\
&R_i \cong \frac{\left(R_\infty - R(0)\right)^2 + \left(R'(0)/\delta\right)^2}{4R_\infty\left(1-R_\infty\right)^2}
\end{aligned}
\qquad \text{A17}
$$

These values may be used as starting estimates for a non-linear least squares best fit to the exact expression, Eq A14. In practice, this method typically yields estimates that are within a few percent of the final optimized values. It is useful to use the estimate for γ to limit the number of points used in a fit when the waveform is strongly damped because there is little information obtained from fitting to just R_∞. We typically truncate the fit when the decay envelope reaches 2% of the $t = 0$ value, so that $t_{max} = 4/\gamma$.

INITIAL DISTRIBUTION
UNLIMITED RELEASE

Scott Chalmers
Film Metrics
10655 Roselle St., Suite G
San Diego, CA 92121

Herman Chui
Hewlett Packard Co.
350 W. Trimble Rd.
San Jose, CA 95131

Kevin Killeen
Hewlett Packard Co.
3500 Deer Creek Rd. - MS 26M7
PO Box 10350
Palo Alto, CA 94303-0867

Rick Stall
EMCORE Corporation
394 Elizabeth Avenue
Somerset, NJ 08873

MS 0601 W. G. Breiland (8)
0601 J. Y. Tsao
0601 M. E. Coltrin
0601 J. Han
0603 P. Esherick
0603 H. Hou
0603 J. Klem
0603 A. Vawter
1077 L. Cecchi
1078 J. McBrayer
1415 E. Chason
1415 J. Floro
1415 W. Gauster
1421 E. Stechel
1427 S. T. Picraux
1436 D. L. Chavez, LDRD Office
9018 Central Technical Files, 8940-2 (1)
0899 Technical Library, 4414 (5)
0619 Review and Approval Desk, 12690, for DOE/OSTI (2)
0161 Patent & Licensing Office, 11500, (3)